Possibility of metastable atomic metallic hydrogen

Craig M. Tenney, Keeper L. Sharkey, and Jeffrey M. McMahon [*]
Department of Physics and Astronomy, Washington State University, Pullman, Washington 99164, USA

Metallic hydrogen is expected to exhibit remarkable physics. However, the pressures at which it is expected to be stable are extremely high relative to current experimental capabilities (static conditions). For practical (and terrestrial) significance, a key question is therefore whether it is metastable. In this work, this possibility is investigated, using first-principles calculations. Particular attention is given to the atomic body-centered tetragonal structures, predicted as being representative of the lowest-pressure stable metallic phase. The results show that, of these, the Cs-IV structure is metastable upon decompression, from molecular dissociation (expected to occur just below 500 GPa) to approximately 250 GPa. Results for structure prediction for metallic phases at lower pressures are also presented. Together, these results suggest that below 200 GPa, metallic hydrogen has no region of stability. All of the approximations used in the calculations are considered, and they are not expected to qualitatively affect the results. Atomic metallic hydrogen is therefore expected to have a (pressure) region of metastability, but the results strongly suggest that the metallic phase (more generally) is not so to zero pressure. These results are expected to provide important information for experiments.

I. INTRODUCTION

In 1935, Wigner and Huntington predicted [1] that sufficient pressure would dissociate hydrogen molecules, and that any Bravais lattice of such atoms would be metallic. (Alternative metallization scenarios will be considered below.) The problem of metallic hydrogen has received considerable attention, as reviewed in Ref. [2]. Initial interest was primarily related to astrophysical problems [3]. Subsequently (and more recently), there has been significant interest in it at relatively low temperatures. This can be attributed to the remarkable properties that are expected. This includes, for example, high-temperature superconductivity [4,5]. The possibility of a zero-temperature liquid ground-state has also been suggested [6]. In this case, hydrogen may have quantum ordered states that represent novel types of quantum fluids [7]. Applications of the (expected) remarkable physics could revolutionize several fields. Possible scientific investigations and technological uses (of metastable solid metallic hydrogen, in particular) have been speculated on in Refs. [8,9].

The pressures required to dissociate hydrogen molecules are expected to be significant [447(3) GPa according to computation [10], consistent with experiment that shows [11] at least above 440 GPa, possibly near 495 GPa [12]]. Particularly important for practical (and terrestrial) significance is therefore whether metallic hydrogen is metastable. This problem was noted by even by Wigner and Huntington [1]. It was not until the 1970s, however, that it would be considered in detail.

The possibility of metastable metallic hydrogen was suggested and most fully considered in 1972 [13,14]. (For references to earlier studies, see Ref. [15].) However, an improved analysis in 1977 [16] disagreed with these [13] results.

Solid metallic hydrogen was soon after considered (by one of the earlier [13] authors) in Ref. [17], again with expectations of a metastable phase. However, somewhat different results were again obtained by others [18] (the cause of which is difficult to judge with certainty). Note that, around the same time, a possible zero-temperature liquid ground-state was also studied [6]. A further analysis [19] concluded that the possibility of such a phase near the metastable zero-pressure point could not be ruled out (conjectured on earlier, in Ref. [13]). Herein, only the possibility of a solid phase will be considered.

The theoretical capabilities available limited early calculations (such as those discussed above) to perturbation theory, incomplete treatment of exchange and correlation effects, and/or consideration of only select (e.g., one- and a few two-atom) crystal lattices. While some justifications were given for both perturbation theory [20] and the approximation of the electron–electron interaction [21], the disagreements (discussed above) call into question the actual uncertainties involved.

Theoretical capabilities have significantly progressed over time. The properties of hydrogen can now be accurately calculated from first principles [2], and crystal-structure prediction plays an important role in materials discovery [22]. Reference [23], for example, confirmed the main part of the results in Ref. [13], using density-functional theory [24]. This includes a minimum on the curve of total energy as a function of volume near ambient pressure, with monoatomic metallic hydrogen having a tendency towards crystallization (at this point) in highly anisotropic structures, and stability with respect to long-wavelength density disturbances at both this and higher pressures. The problem of metastable metallic hydrogen was also considered more recently in Ref. [25]. The energetic stability of a set of candidate structures consisting of (relatively-)recently proposed [25–28] ground-state and

[*] jeffrey.mcmahon@wsu.edu

low-lying metastable phases of dense hydrogen at zero pressure was studied, including their relationship (transition paths and the associated energy barriers) to the molecular phase. The results of this work are discussed in context below. The answer to the question of whether or not the metastable phase exists still remains to be answered in full.

The answer to this question presupposes a solution to a series of interrelated problems. (1) Determination of the minimum-energy crystal structure(s). This includes proof that they lie at stationary points (with respect to all parameters). (2) Proof of lattice stabilities. This includes with respect to both homogeneous and all other infinitesimal deformations. (3) Analysis of the relationship between the ground- and metastable-state structure(s) (assuming that such exist), and to the molecular phase. This includes an analysis of the processes that are undergone during transitions between them, and also when the pressure is removed. (4) Determination of the lifetime. This includes stability with respect to both quantum and thermal fluctuations.

In this paper, the possibility of metastable metallic hydrogen is investigated, using first-principles calculations. The answer to the question of whether or not this phase exists is answered in full, including both at relatively low (to zero) pressures and higher. All approximations used in the calculations are considered.

The remainder of this paper is outlined as follows. A description of the methods used is presented next. Then are the results. Particular focus is given to problems (1) and (2) (discussed above), and problem (3) is indirectly considered. A discussion follows. This includes a thorough consideration to problem (4). Conclusions and an outlook end this discussion. Reference [29] (see, also, Refs. [30–41] therein) accompanies this work.

II. METHODS

A. Electronic-structure calculations

All calculations were performed using the QUANTUM ESPRESSO (QE) density-functional theory [24] (see Ref. [29], Sec. II C 1 for a justification for this approximation) code [42]. The pseudopotential approximation (for a justification for this, see Ref. [28]) based on the projector augmented-wave method [43] was used [44] to replace the bare Coulomb potential of the protons. The Perdew–Burke–Ernzerhof generalized gradient approximation exchange–correlation functional [45] was used. QE is based on a plane-wave basis set, and kinetic-energy cutoffs of 57.5 Ry for the wave function and 345.5 Ry for charge density and potential were used. For Brillouin-zone sampling, at least $32 \times 32 \times 32$ (unshifted) wave-vector **k** points were used. (See Ref. [29], Sec. II D 1 for a further discussion of convergence.) The smearing scheme of Methfessel–Paxton [46] was used for Brillouin-zone integrations, with a smearing width of 0.02 Ry. These choices give a total convergence, in energy, for example, to better than 0.5 meV/proton.

B. Geometry optimizations

Stationary points of structures were found by performing constant-pressure geometry optimizations. These were done using the Broyden–Fletcher–Goldfarb–Shanno algorithm [47], as implemented within QE. Energies, forces, and pressures were converged to 10^{-5} Ry, 10^{-4} Ry/a.u., and 0.5 kbar, respectively.

C. Structure prediction

Searches for stable structures of metallic hydrogen were performed using *ab initio* random structure searching [48]. This is a robust approach that has been used previously to find structures of both molecular [27,49,50] and atomic [28] hydrogen that are consistent with experiment.

Calculations were performed using electronic-structure calculations and geometry optimizations, as described above. For the former, the basis-set cutoffs were reduced to 46 and 221 Ry, respectively, and the Brillouin-zone sampling to $8 \times 8 \times 8$ (shifted) **k** points. For the latter, the energy and force convergence-criteria were relaxed by an order of magnitude. These values are (essentially) the default ones, capable of generating candidate structures for further analysis.

Random structures were constructed by first generating random primitive (lattice) vectors, renormalizing the volume (to the expected average), and then generating random proton configurations. Searches were done over unit cells containing 1 to 10 atoms. Geometry optimizations (at zero pressure) were performed. For each unit-cell size, 1000 trials were considered. The symmetries of the (relaxed) structures were determined using the FINDSYM program [51].

D. Lattice stabilities

Phonons were calculated using density-functional perturbation theory, as implemented within QE. (Section IV provides a justification for the harmonic approximation, and discusses the possible influence of nuclear quantum motion on the calculated results.) Each (phonon) density of states $F(\omega)$ was calculated from the minimum to maximum phonon energies, in steps of 1 cm^{-1}. Grids of phonon wave vectors **q** at least as dense as $4 \times 4 \times 4$ were used for these calculations. (See Ref. [29], Sec. II D 2 for a discussion of convergence.)

III. RESULTS

It is unclear whether the first (lowest-pressure) metallic phase (and as a good metal) of hydrogen will be molecular or atomic. It was initially thought [1] that metallization of hydrogen would occur by molecular dissociation. Later calculations [52] suggested that this may instead occur at lower pressures (in the molecular phase). Neither scenario is yet agreed on as correct.

Experiments suggest [53], however, that if the indirect band gap closes, initially insulating and then semiconducting molecular hydrogen will first transform to a semimetal. This suggestion appears consistent with behavior seen in recent experimental measurements [11] of the temperature dependence of the electrical conductivity above 350–360 GPa; though, infrared (IR) spectroscopy measurements [54] suggest a transition to a phase (called H_2-PRE) near this pressure, with reflected and transmitted light indicating that it is most likely semiconducting. Other recent measurements [55] show a discontinuous change to zero in the integrated transmitted
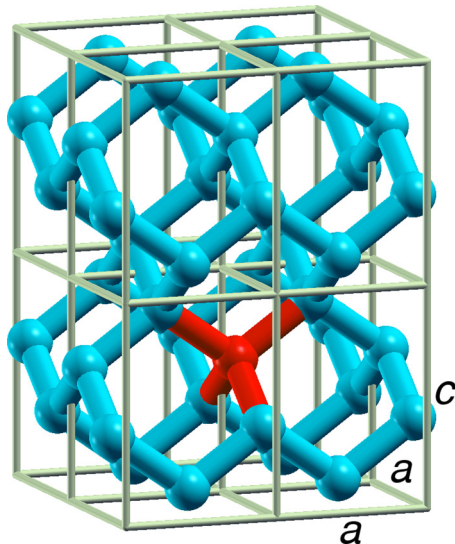
FIG. 1. Body-centered tetragonal (BCT) structure ($I4_1/amd$ space group) of atomic metallic hydrogen. Shown is a $2 \times 2 \times 2$ super-cell. Note the tetragonal coordination of the atoms (the lower central atom is highlighted). (Fictitious bonds are shown for clarity.) Note also the square base ($a \times a$) and unequal height ($c \neq a$).

FIG. 2. Phase diagram (at 0 K) of the BCT structures, below molecular dissociation. Enthalpies (static) ΔH_{static} [defined in a term of E_{static} in Eq. (1)] are shown relative to Cs-IV as a function of pressure P (calculated every 50 GPa). Three (qualitative) regions of stability are separated by dotted lines and labeled a, b, and c. Up and down arrows are used to indicate where the β-Sn and $c/a \ll 1$ structures, respectively, become the most stable. The latter arrow also points to where the β-Sn, diamond, and Cs-IV structures become degenerate in enthalpy.

intensity over the IR range near 425 GPa (a result confirmed by Ref. [54]). While this is a necessary condition for the infrared observation of metal hydrogen though, it is not definitive evidence (see the discussion in both Refs. [54,55]). Note that if a semimetallic phase is confirmed (e.g., through additional measurements), depending on the structure, such a phase may not be a conventional semimetal [56]. Altogether, it is still unclear whether molecular hydrogen will become a good metal, prior to dissociation. Note that this discussion does not include suggestions of (semi)metallization in relation to phases discovered at higher [e.g., room [57] (see also Ref. [58]) and above [59]] temperatures.

There is little doubt that metallization will occur with enough pressure though. And, as mentioned above, it has been shown [1] that any Bravais lattice of hydrogen atoms will be metallic. In considering metastable metallic hydrogen, it therefore seems most reasonable to consider atomic and mixed atomic–molecular structures.

A. Body-centered tetragonal structures

The most promising candidate structures for metastable metallic hydrogen (at least at higher pressures) are the most stable ones just above molecular dissociation. While these are not known experimentally, first-principles calculations [28] suggest that they can be represented by a body-centered tetragonal (BCT) structure (possibly including lower-symmetry distortions [25]), as shown in Fig. 1.

In the BCT representation, there are five structures of note (in atomic hydrogen), defined by the axial ratio c/a; three of these have been considered before, those of β-Sn ($c/a < 1$), diamond ($c/a = \sqrt{2}$), and Cs-IV ($c/a > 1$), and the other two have $c/a \ll 1$ and $\gg 1$. Their structural parameters are reported in Ref. [29], Sec. I A 1. An analysis of (only) these
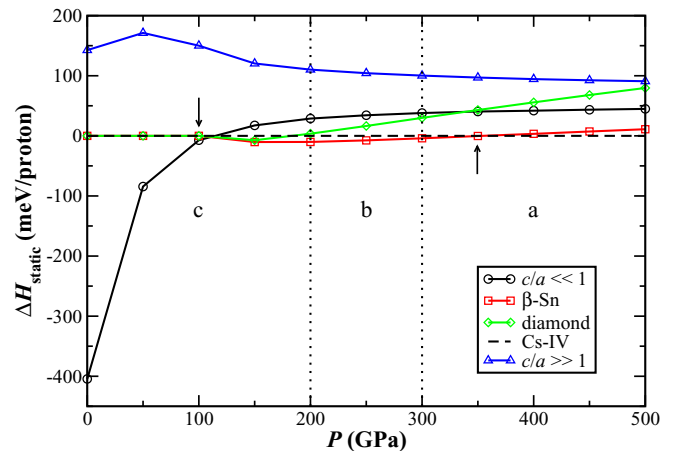
structures reveals several general qualitative features about metastable metallic hydrogen.

Consider the phase diagram (at 0 K) below molecular dissociation, shown in Fig. 2. The pressure range can be (qualitatively) divided into three regions.

(a) >300 GPa: the relative enthalpies of most of the structures remain relatively flat. The only exception to this is the diamond structure (discussed in more detail below).

(b) 200–300 GPa: the enthalpies of the β-Sn, diamond, and Cs-IV structures become nearly degenerate, whereas those with $c/a \ll 1$ and $\gg 1$ begin to decrease and increase, respectively.

(c) <200 GPa: the β-Sn, diamond, and Cs-IV structures become degenerate (precisely at 100 GPa), whereas those with $c/a \ll 1$ and $\gg 1$ sharply decrease and increase, respectively.

This division is supported by the results of additional calculations, presented and discussed below and in Ref. [29], Sec. I B 1.

Additional insight (including into Fig. 2) is obtained by considering the energy of the BCT structure over the entire range of c/a, shown in Fig. 3.

As will be supported by the results of additional calculations (below), there are two especially important points that are suggested by these results.

(1) There is a collapse of energy barriers in the potential-energy surface (PES) of (atomic) metallic hydrogen, between 300 and 200 GPa. Consider the diamond structure. At relatively high pressures, this structure forms an energy barrier (a maximum) between those of β-Sn and Cs-IV. Figure 2 shows that its relative enthalpy decreases continuously with decreasing pressure. Between 300 and 200 GPa, its relative energy decreases appreciably. By 100 GPa, it has collapsed completely, leaving only a single minimum in this region of c/a ($\approx \sqrt{2}$). Note in Fig. 2 that the β-Sn, diamond, and Cs-IV
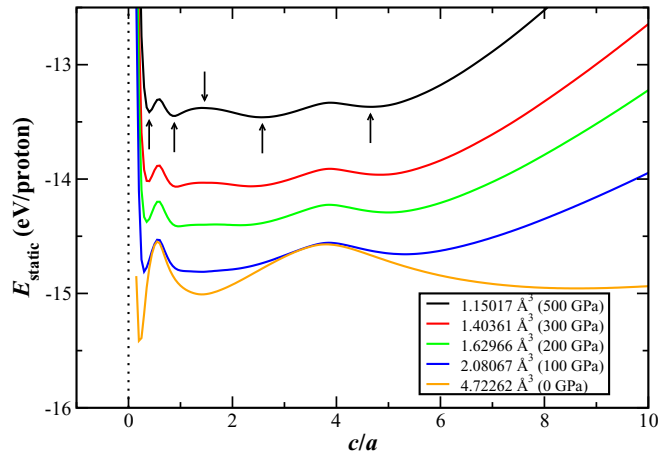
FIG. 3. Energies (static) E_{static} [defined in Eq. (1)] of the BCT structure as a function of the axial ratio c/a (calculated every 0.05). A dotted line is used to indicate $c/a = 0$. Fixed volumes are shown, calculated by the average of each structure at the pressure indicated in parentheses. The $c/a \ll 1$, β-Sn ($c/a < 1$), diamond ($c/a = \sqrt{2}$), Cs-IV ($c/a > 1$), and $c/a \gg 1$ structures are indicated with arrows (in order of increasing c/a) at 500 GPa.

structures become degenerate in enthalpy at this pressure. The stability of the diamond structure is further discussed in Ref. [29], Sec. I C 1.

(2) There is a tendency towards the formation of molecules, below 200 GPa. Consider the structures with $c/a \ll 1$ and $\gg 1$. The sharp increases in energy as $c/a \to 0$ and $\to \infty$ are due to the Coulomb repulsion between protons (in the primitive cell and its images) that approach each other (assuming a homogeneous negative background). In the present case (i.e., considering only the primitive cell), this leads to one-dimensional chains of protons along c or a, respectively. Considering only two protons (one in the primitive cell and a single image) though suggests that the energy minima prior to the sharp increases may be a result of a tendency towards the formation of molecules. Note the sharp decrease in energy of the $c/a \ll 1$ structure, and the nearest-neighbor distance (at zero pressure) of 0.9900 Å. This suggestion is confirmed by considering supercells (in which such molecule formation can occur) of analogous atomic structures (Sec. III B), which are found to relax to (completely) molecular ones (these results are presented and discussed in Ref. [29], Sec. I C 2).

The ability of atoms to approach each other is the result of the collapse of atomic energy barriers (discussed above). While this occurs, so does a hardening of molecular ones. Note the relative heights (and their trends with pressure) of the maxima separating the $c/a \ll 1$ and $\gg 1$ structures from the atomic ($c/a \approx \sqrt{2}$) region. These results are consistent with those [25] for a set of phases of dense hydrogen (including Cs-IV) in the limit of zero pressure, that there is *no* transition barrier that can be detected along the transformation path to diatomic molecular structures.

B. Structure prediction

While the BCT structures (discussed above) are the most promising candidates for metastable metallic hydrogen at

pressures near molecular dissociation, there is no guarantee that they are representative of those (potentially) so at lower pressures.

Consider the lattice energy $E_{lattice}$ of metallic hydrogen; in the adiabatic approximation (for a justification for this, see Ref. [29], Sec. II C 3):

$$E_{lattice} = E_{static} + E_{vib}, \tag{1}$$

where E_{static} is the static (electronic ground-state energy, with a fixed lattice) contribution and E_{vib} is that resulting from atomic vibrations. In metallic hydrogen (and unlike ordinary metals), E_{static} favors anisotropic structures; see Ref. [13] for a discussion of this. E_{vib}, however, favors symmetric ones. The subtle (and important) details of these terms, including their relative magnitudes, depend on the pressure. At low pressures, $E_{lattice}$ is determined largely by E_{static}. The relative magnitude of E_{vib} is small, and it varies smoothly with changing ion configuration (i.e., it depends little on the structure) [13]. (This is verified in Ref. [29], Sec. I B 4, for the most stable atomic structures considered below.) It is with increasing pressure that E_{vib} becomes (especially) important [28].

Searches were performed for metallic (atomic and mixed atomic-molecular) structure(s) with the lowest values of E_{static} at zero pressure. These revealed several candidate structures. An analysis of the most stable ones over the entire pressure range further supports the results above; details are provided in Ref. [29], Sec. I B 1. For this discussion, it is relatively low pressures that are of main interest.

Below 200 GPa, the structures found show a tendency towards the formation of molecules. This is consistent with Point (2), as suggested by Fig. 2 (discussed above). It is supported though by a detailed analysis (below) of the structures themselves.

In searches with more than a few atoms, mostly molecular or mixed atomic–molecular structures were found. In addition, for the latter, as the number of atoms in the search increased, a greater proportion of molecules to atoms were found. This trend is also reflected in the relative enthalpies, presented in Ref. [29], Sec. I B 1. That this trend occurs indicates that such structures may not be at stable stationary points.

The results above suggest that any metastable structure(s) of metallic hydrogen are (completely) atomic. Such were found in searches with a few or less atoms. The most stable (and nearly degenerate in energy) ones are shown in Fig. 4. Note that they are all very similar in their symmetries.

The tendency towards the formation of molecules can be seen, even in these structures. Note the close proximity of atoms (into the page), which is approximately 0.9914 Å. This is analogous to the results for the BCT $c/a \ll 1$ structure (discussed above). This also indicates that these structures may not be at stable stationary points (confirmed, in results presented below). Further results and discussion are provided in Ref. [29], Sec. I B 3.

C. Lattice stabilities

A crystal lattice is stable if, for infinitesimal deformations, atoms return to their assumed equilibrium positions. By solving the equations of motion for the normal modes of vibration,
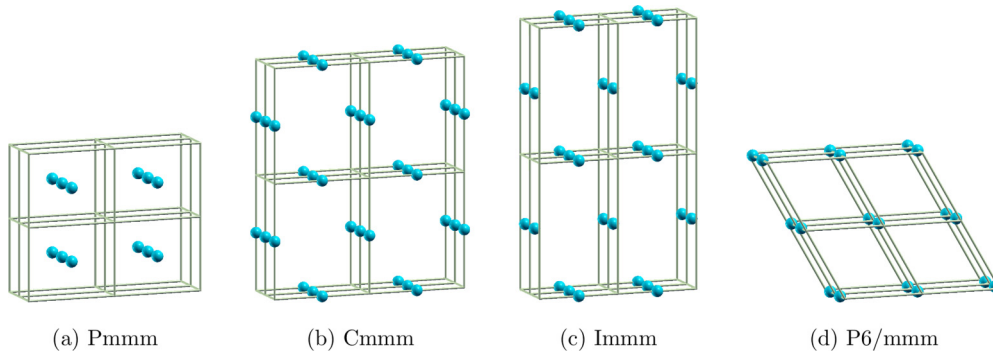
(a) Pmmm   (b) Cmmm   (c) Immm   (d) P6/mmm

FIG. 4. Most stable candidate structures of metastable (atomic) metallic hydrogen, at zero pressure. Shown are $2\times2\times2$ supercells. Their space groups are specified in the subcaptions.

this is equivalent to the condition that their frequencies ω satisfy:

$$\omega_j(\mathbf{q}, s)^2 \geqslant 0$$

for all phonon branches j, where $\mathbf{q}$ is the wave vector and s is a label denoting the polarization [60]. (In other words, they are real; for an imaginary frequency means that the system, subject to a small displacement, will disrupt exponentially with time.) This includes both homogeneous deformations (elastic stability), described by long-wavelength ($\mathbf{q} \to \mathbf{0}$) phonons, and all other infinitesimal ones (dynamical stability). The stabilities were determined by calculating the phonon density of states $F(\omega)$ over all ω (along both the real and imaginary axes), for each structure.

Consider first the BCT structures; Fig. 5 shows the $F(\omega)$ of Cs-IV. Note that all other such structures are unstable; see Ref. [29], Sec. I C 1, for results and a discussion about β-Sn.

Figure 5(a) shows the $F(\omega)$ for pressures from 500 (down) to 250 GPa. The absence of imaginary frequencies proves stability (at least to approximately these pressures). Consider also the (qualitative) changes in the spectra. Down to 350 GPa, they (mostly) retain their shape, with frequencies simply shifting to lower values. Such a behavior is expected for a structure

that remains qualitatively the same (in terms of its underlying PES). However, by 250 GPa, while there continues to be a shift to lower frequencies, differences become apparent.

Figure 5(b) shows the $F(\omega)$ for pressures below 250 GPa. By 200 GPa, a small instability appears, which increases with decreasing pressure. However, the spectra remain (qualitatively) similar (at least until zero pressure). This behavior, along with that seen in Fig. 5(a) (discussed above), is consistent with a transition region between 300 and 200 GPa, where the underlying PES of hydrogen changes significantly.

Phonon dispersion relations and elastic constants of Cs-IV near the (pressure) limit of metastability (250 and 200 GPa) are presented and discussed in Ref. [29], Sec. I C 1. Considered together, the results show that the structure is near the limits of both dynamic and elastic stabilities at 250 GPa. By 200 GPa, both dynamical and elastic instabilities have occurred.

Consider now the candidate structures; Fig. 6 shows $F(\omega)$ of those shown in Fig. 4. They exhibit very similar spectra (as expected, given their similarities). Note though their tails that extend to very high imaginary frequencies. Although these have significantly smaller relative magnitudes, an expanded view reveals peaks. Therefore, while these structures are at
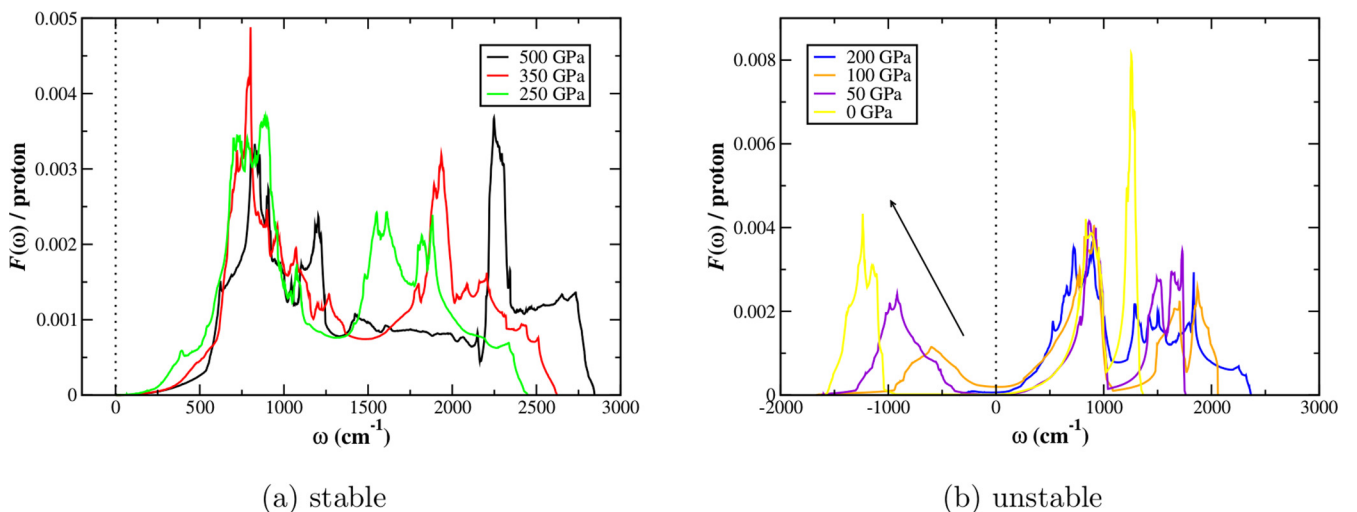

(a) stable

(b) unstable

FIG. 5. Phonon density of states $F(\omega)$ of the Cs-IV structure. Several pressures are shown, and are separated by regions of (a) stability and (b) instability. The dotted lines are used to separate the stable (real) from unstable (imaginary) phonon frequencies (shown as negative values). Note that there are no imaginary frequencies in (a). The arrow in (b) highlights the increasing instability with decreasing pressure.
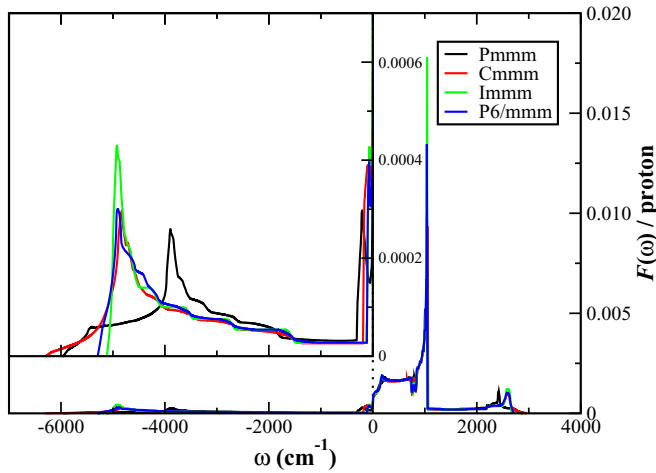
FIG. 6. $F(\omega)$ of the candidate (atomic) structures (Fig. 4), at zero pressure. A dotted line is used to separate the stable from unstable frequencies. The inset shows the imaginary-frequency region.

stationary points, they are unstable ones. This is further supported by additional results, provided in Ref. [29], Sec. I C 2. Note that the stabilities of these structures at higher pressures are also presented and discussed therein.

IV. DISCUSSION

The possibility of metastable metallic hydrogen was investigated in detail. This was considered from two approaches: an analysis of the BCT structures (stable above molecular dissociation), and the prediction and analysis of candidate ones at zero pressure. The results obtained are self-consistent, and provide strong evidence regarding this possibility.

The results are concisely summarized by the processes undergone on the PES of hydrogen, as the pressure is removed (following molecular dissociation). (a) At (relatively) high pressures (>300 GPa): the PES of (atomic) metallic hydrogen is well defined. It remains qualitatively similar below molecular dissociation. (b) At intermediate pressures (200–300 GPa): the energy barriers of metallic hydrogen on the PES collapse, whereas those of the (completely) molecular phase harden. (c) At low pressures (<200 GPa): the PES of molecular hydrogen is well defined. From these results, it is concluded that (atomic) metallic hydrogen is metastable, but only to 300–200 GPa. Below 200 GPa, metallic hydrogen has no region of stability.

Because calculations were carried out with a focus on the metallic phase, the relationship to the molecular one [problem (3)] was not considered directly. In order to obtain insight into this, it is necessary to consider whether any approximations in the computational methods and approach would affect the two phases differently. This is especially important at pressures near and below the limit of metastability. Approximations for the metallic phase were already considered in detail, and justified above and in Ref. [29], Sec. II C. For the molecular phase, and the relationship between the two though, there are additional considerations.

The primary approximation (especially as would affect the results) made in density-functional theory is the choice of

exchange–correlation functional. (Largely) because of self-interaction errors [61], semilocal functionals (as the one used herein) tend to underestimate band gaps. This should result in a slight overestimate of the stability of the metallic phase. However, as long as the calculated band gap does not close while the true one remains finite, the accuracy is expected to be reasonable. This is the case for the relevant molecular phase, where the predicted [27] stable structure ($C2/c$) does not become metallic until about 300 GPa.

The relationship between the metallic and molecular phases is described by any energy barrier(s) separating them. Consider first a (very) simplified description of the transition between them, using the (simplest, and relevant) molecule H_2^+. While functionals describe the chemical bond well, they fail dramatically as the molecule is stretched. This is caused by delocalization error (in this system, at the dissociation limit, the hydrogen atoms are each assigned half of an electron, and the total energy is much too low). Returning to the solid state: In the limit of zero pressure, calculations [25] do not show *any* energy barrier between metallic and molecular hydrogen (discussed above). And an insightful analysis [62] into limitations of density-functional theory implies that, even with delocalization error, it seems unlikely that an additional energy barrier can be predicted by an exact theory when none can be detected by the current one. Therefore it seems likely that any energy barrier(s) of metallic hydrogen do (fully) collapse between zero pressure and around the intermediate range (where the theory describes the metallic phase well).

There is a range of pressures where this relationship may also depend on quantum nuclear statistics. At low pressures, anisotropic intermolecular interactions between hydrogen molecules are weak. Because of this, the angular momentum of an individual molecule remains a good quantum number. (Para)hydrogen molecules freely rotate about their centers of mass. As the pressure is increased to 110 GPa [63], the rotational symmetry is broken, and hydrogen transitions to phase II. Therefore the structure of phase II is determined by the zero-point rotational energy (and thus depends on the total spin) of the molecules.

A quantitative description (of phase II) is still lacking. Relatively recent simulations even suggest that this phase cannot be described in terms of a single classical structure [64]. Nonetheless, qualitatively consistent structures can be found (e.g., the 24-atom $P2_1/c$ structure reported in Ref. [49]). This suggests that static-lattice calculations can at least determine reasonable energy barriers. Since the results (above) depend on these, quantum nuclear statistics are therefore not expected to significantly affect any conclusions drawn from them.

With the computational methods and approach considered in detail for both the atomic (Sec. II) and molecular (above) phases, a final (significant) consideration is the influence of nuclear quantum motion. Lattice stabilities (presented above and Ref. [29], Sec. I C) including vibrational energies (Ref. [29], Sec. I B 4) were calculated within the harmonic approximation [60]. Corrections to this as applied to lattice stabilities could be important, because metastability is ultimately determined by their consideration.

Corrections to the harmonic approximation (and as applied to metallic hydrogen) have been studied in Ref. [65]. If the phonon frequencies are well behaved (i.e., no modes with

anomalously low or imaginary frequencies), then corrections change them only quantitatively. This is consistent with recent calculations [66] that considered anharmonic effects on the lattice stability of the Cs-IV structure near 500 GPa. If the phonon frequencies are not well behaved, however, it is possible for corrections to raise them and stabilize the lattice.

These considerations narrow the range over which, and provide insight into where anharmonic effects may be significant. At higher pressures, the phonon frequencies of the Cs-IV structure are well behaved [down to 250 GPa—Fig. 5(a)]; at lower pressures, there does not appear to be an energy barrier for the metallic phase (discussed above). Therefore these effects would (if at all) be most important at intermediate pressures. For the Cs-IV structure though, calculations of the elastic constants (Ref. [29], Sec. I C 1) show that it becomes unstable due to an elastic instability between 250–200 GPa. Therefore, if anharmonic effects are significant, they involve a transition from this structure to one that is stabilized by these.

The energy landscape including the Cs-IV structure provides insight into possible structural transitions. Note that the static-lattice landscape is approximation free (in this context); ions move on this (even at 0 K) as zero-point motion. Consider (again) the landscape for the BCT structure as a function of c/a (Fig. 3). The β-Sn, diamond, and Cs-IV structures are connected over a region that can be described as one where many local optima exist (the locations of these structures), when viewed at a course level leads to a global optimum (the diamond structure—which becomes an actual minimum at lower pressures). This description is common in metals with large electron–phonon coupling (expected for metallic hydrogen [4]), where structures are (in the absence of anharmonic contributions) destabilized by this interaction [67]. When this occurs in more symmetrical structures (such as diamond), it can result in distorted (lower-symmetry) ones in which the electronic density of states at the Fermi level is reduced. When nuclear quantum motion is considered, the energy landscapes become smoother (closer to the "course level") and hence much simpler [68]; this result can be understood, using the path-integral formulation of quantum mechanics [69]. Therefore the diamond structure may have a narrow range of stability over pressures near the limit of metastability.

Metastable metallic hydrogen, even at its stable pressures, may have important practical significance. Such pressures are much less than those for which hydrogen is expected to remain molecular [10–12]. They are even less than those for which recent electrical measurements [11] indicate insulating behavior in the molecular phase (up to approximately 360 GPa).

Whether this phase is even realizable though depends on its lifetime. The major question is the mechanism by which the first few nucleations (from atoms in the atomic metal to molecules) takes place, and the probable time that will elapse before this occurs. Once this does occur, the transition to the molecular phase is expected to be fast. There are two primary sources of this nucleation, which are considered separately below.

Crystal surfaces and (interior) defects are obvious regions for this to occur. Evaporative recombination rates from surfaces at zero temperature, due to quantum mechanical tunneling and also by thermal effects were studied in Ref. [70].

Lifetimes at zero pressure were estimated to be very short (less than approximately 10^{-3} s). Even a small amount of pressure though increases this enormously. It has also been suggested [13] that stability against this could be attained by covering the sample with a specially chosen substance. As for defects, it seems that a crystal of metallic hydrogen free of such could be obtained at high pressures, and maintained throughout decompression. A method for calculating the formation energy of localized defects in crystalline solids, which permits relaxation of all particle positions and Einstein frequencies, was proposed in Ref. [71]. For metallic hydrogen, it was shown that dynamical relaxation does not upset the stability of the system to vacancy formation, for example.

Zero-point motion or thermal vibrations of the atoms in the bulk must also be considered. Reference [72] suggested that the former alone will lead to nucleation at zero pressure, within the order of 10^{-3} s. Again under pressure though, the lifetime is increased. Reference [73] noted that the former result may not be completely reliable anyway, as the effects of screening were not properly accounted for. Doing so leads to speculation that three or more protons may be required in order for recombination to occur (which is a more rare fluctuation). Pair- and three-proton interactions were considered more recently in Ref. [74]. It was found that the probability of protons coming together depends essentially on the electron gas density (or pressure). With this increasing, the probability of multiproton tunneling sharply decreases. A more recent consideration of nucleation in the bulk was in Ref. [75]. The decay of the metallic phase as the pressure is relieved below molecular dissociation was considered. It was found that the metallic state is expected to be long lived down to about 10–20 GPa, and then it decays instantly at lower pressures. The latter is (essentially) consistent with a result of Ref. [76], that the Cs-IV structure (starting at only 10 K) has a lifetime of order 40 fs at ambient pressure. The analysis in Ref. [75], however, was based on the assumption that the state of the system is completely determined with the density; as shown herein, energy barriers for metallic hydrogen have already collapsed at much higher pressures. In addition, the tunneling transition between phases was analyzed semiclassically [77].

It seems that a quantitative determination of the lifetime of the metastable phase remains an open question. Answering this would require more sophisticated approaches than those discussed above. Even with the more approximate methods though, it is expected that the lifetime of this phase is significant (such that it is long lived) under pressure (also noted in Ref. [13]). Based on the results presented herein, this is the important region anyway.

The pressures at which metallic hydrogen has been predicted to be metastable can be achieved under static (diamond anvil cell) conditions [78]. Since it is expected to be long lived at these pressures (as just discussed), these results should provide important information for, and be verified by experiments. This is particularly timely, with recent claims [12] of the realization of (ground-state) atomic metallic hydrogen at low temperatures in static experiments.

The answer to the question of whether or not metastable metallic hydrogen exists has been answered in full. There

are still several important and open questions though. Perhaps most so involve the properties of this phase. Such will determine its possible scientific and technological uses [8,9]. Studying these and answering other such questions will be the subjects of future work.

[1] E. Wigner and H. B. Huntington, J. Chem. Phys. **3**, 764 (1935).

[2] J. M. McMahon, M. A. Morales, C. Pierleoni, and D. M. Ceperley, Rev. Mod. Phys. **84**, 1607 (2012).

[3] I. Baraffe, G. Chabrier, and T. Barman, Rep. Prog. Phys. **73**, 016901 (2010).

[4] N. W. Ashcroft, Phys. Rev. Lett. **21**, 1748 (1968).

[5] J. M. McMahon and D. M. Ceperley, Phys. Rev. B **84**, 144515 (2011).

[6] K. K. Mon, G. V. Chester, and N. W. Ashcroft, Phys. Rev. B **21**, 2641 (1980).

[7] E. Babaev, A. Sudbo, and N. W. Ashcroft, Nature (London) **431**, 666 (2004).

[8] W. J. Nellis, Philos. Mag. Part B **79**, 655 (1999).

[9] W. J. Nellis, J. Phys.: Condens. Matter **29**, 504001 (2017).

[10] J. McMinis, R. C. Clay, D. Lee, and M. A. Morales, Phys. Rev. Lett. **114**, 105305 (2015).

[11] M. I. Eremets, A. P. Drozdov, P. P. Kong, and H. Wang, Nat. Phys. **15**, 1246 (2019).

[12] R. P. Dias and I. F. Silvera, Science **355**, 715 (2017).

[13] E. G. Brovman, Y. Kagan, and A. Kholas, J. Exp. Theor. Phys. **34**, 1300 (1972).

[14] Y. M. Kagan and E. G. Brovman, Sov. Phys. Usp. **14**, 809 (1972).

[15] L. G. Caron, Comments Sol. State Phys. **6**, 103 (1975).

[16] F. E. Harris and J. Delhalle, Phys. Rev. Lett. **39**, 1340 (1977).

[17] Y. Kagan, L. A. Maksimov, and A. E. Trenin, Zh. Eksp. Teor. Fiz. **75**, 1729 (1978).

[18] V. V. Avilov and S. V. Iordanskiĭ, Fiz. Tverd. Tela **19**, 3516 (1977).

[19] S. Chakravarty and N. W. Ashcroft, Phys. Rev. B **18**, 4588 (1978).

[20] Y. Kagan, V. V. Pushkarev, and A. Kholas, Zh. Eksp. Teor. Fiz. **73**, 967 (1977).

[21] E. G. Brovman, Y. Kagan, A. Kholas, and V. V. Pushkarev, Zh. Eksp. Teor. Fiz. Pis. Red. **18**, 269 (1973).

[22] L. Zhang, Y. Wang, J. Lv, and Y. Ma, Nat. Rev. Mater. **2**, 17005 (2017).

[23] E. Maksimov and D. Savrasov, Solid State Commun. **119**, 569 (2001).

[24] R. O. Jones, Rev. Mod. Phys. **87**, 897 (2015).

[25] H. Y. Geng, H. X. Song, J. F. Li, and Q. Wu, J. Appl. Phys. **111**, 063510 (2012).

[26] K. A. Johnson and N. W. Ashcroft, Nature (London) **403**, 632 (2000).

[27] C. J. Pickard and R. J. Needs, Nat Phys **3**, 473 (2007).

[28] J. M. McMahon and D. M. Ceperley, Phys. Rev. Lett. **106**, 165302 (2011).

[29] See Supplemental Material at http://link.aps.org/supplemental/10.1103/PhysRevB.102.224108 for supplemental results and methods.

[30] M. Born and R. Oppenheimer, Ann. Phys. **389**, 457 (1927).

[31] R. Golesorkhtabar, P. Pavone, J. Spitaler, P. Puschnig, and C. Draxl, Comput. Phys. Commun. **184**, 1861 (2013).

[32] Y. Hinuma, G. Pizzi, Y. Kumagai, F. Oba, and I. Tanaka, Comput. Mater. Sci. **128**, 140 (2017).

[33] H. Liu, H. Wang, and Y. Ma, J. Phys. Chem. C **116**, 9221 (2012).

[34] R. J. Needs, M. D. Towler, N. D. Drummond, and P. L. Ríos, J. Phys.: Condens. Matter **22**, 023201 (2010).

[35] P. E. Blöchl, O. Jepsen, and O. K. Andersen, Phys. Rev. B **49**, 16223 (1994).

[36] M. A. Morales, J. M. McMahon, C. Pierleoni, and D. M. Ceperley, Phys. Rev. B **87**, 184107 (2013).

[37] R. C. Clay, J. Mcminis, J. M. McMahon, C. Pierleoni, D. M. Ceperley, and M. A. Morales, Phys. Rev. B **89**, 184106 (2014).

[38] F. Mouhat and F.-X. Coudert, Phys. Rev. B **90**, 224104 (2014).

[39] M. A. Morales, C. Pierleoni, and D. M. Ceperley, Phys. Rev. E **81**, 021202 (2010).

[40] W. Kohn, Phys. Rev. Lett. **2**, 393 (1959).

[41] T. H. K. Barron and M. L. Klein, Proc. Phys. Soc. **85**, 523 (1965).

[42] P. Giannozzi, S. Baroni, N. Bonini, M. Calandra, R. Car, C. Cavazzoni, D. Ceresoli, G. L. Chiarotti, M. Cococcioni, I. Dabo, A. D. Corso, S. de Gironcoli, S. Fabris, G. Fratesi, R. Gebauer, U. Gerstmann, C. Gougoussis, A. Kokalj, M. Lazzeri, L. Martin-Samos, N. Marzari, F. Mauri, R. Mazzarello, S. Paolini, A. Pasquarello, L. Paulatto, C. Sbraccia, S. Scandolo, G. Sclauzero, A. P. Seitsonen, A. Smogunov, P. Umari, and R. M. Wentzcovitch, J. Phys.: Condens. Matter **21**, 395502 (2009).

[43] G. Kresse and D. Joubert, Phys. Rev. B **59**, 1758 (1999).

[44] pseudopotential: H.pbe-kjpaw_psl.0.1.upf, http://www.quantum-espresso.org/, accessed on 2017-09-04.

[45] J. P. Perdew, K. Burke, and M. Ernzerhof, Phys. Rev. Lett. **77**, 3865 (1996).

[46] M. Methfessel and A. T. Paxton, Phys. Rev. B **40**, 3616 (1989).

[47] R. Fletcher, *Practical Methods of Optimization*, 2nd ed. (Wiley-Interscience, New York, NY, 1987).

[48] C. J. Pickard and R. J. Needs, J. Phys.: Condens. Matter **23**, 053201 (2011).

[49] C. J. Pickard and R. J. Needs, Phys. Status Solidi (b) **246**, 536 (2009).

[50] B. Monserrat, R. J. Needs, E. Gregoryanz, and C. J. Pickard, Phys. Rev. B **94**, 134101 (2016).

[51] H. T. Stokes and D. M. Hatch, J. Appl. Cryst. **38**, 237 (2005).

[52] D. E. Ramaker, L. Kumar, and F. E. Harris, Phys. Rev. Lett. **34**, 812 (1975).

[53] C.-S. Zha, Z. Liu, and R. J. Hemley, Phys. Rev. Lett. **108**, 146402 (2012).

[54] R. P. Dias, O. Noked, and I. F. Silvera, Phys. Rev. B **100**, 184112 (2019).

[55] P. Loubeyre, F. Occelli, and P. Dumas, Nature (London) **577**, 631 (2020).

[56] I. I. Naumov and R. J. Hemley, Phys. Rev. Lett. **117**, 206403 (2016).

[57] M. I. Eremets and I. A. Troyan, Nat. Mater. **10**, 927 (2011).

[58] W. J. Nellis, A. L. Ruoff, and I. F. Silvera, arXiv:1201.0407.

[59] C.-s. Zha, H. Liu, J. S. Tse, and R. J. Hemley, Phys. Rev. Lett. **119**, 075302 (2017).

[60] M. Born and K. Huang, *Dynamical Theory of Crystal Lattices*, International Series of Monographs on Physics (Clarendon Press, Oxford, UK, 1954).

[61] J. P. Perdew and A. Zunger, Phys. Rev. B **23**, 5048 (1981).

[62] A. J. Cohen, P. Mori-Sánchez, and W. Yang, Science **321**, 792 (2008).

[63] H. E. Lorenzana, I. F. Silvera, and K. A. Goettel, Phys. Rev. Lett. **64**, 1939 (1990).

[64] G. Geneste, M. Torrent, F. Bottin, and P. Loubeyre, Phys. Rev. Lett. **109**, 155303 (2012).

[65] H. Beck and D. Straus, Helv. Phys. Acta **48**, 655 (1975).

[66] M. Borinaga, I. Errea, M. Calandra, F. Mauri, and A. Bergara, Phys. Rev. B **93**, 174308 (2016).

[67] P. B. Allen and M. L. Cohen, Phys. Rev. Lett. **29**, 1593 (1972).

[68] I. Errea, F. Belli, L. Monacelli, A. Sanna, T. Koretsune, T. Tadano, R. Bianco, M. Calandra, R. Arita, F. Mauri, and J. A. Flores-Livas, Nature (London) **578**, 66 (2020).

[69] R. P. Feynman, Rev. Mod. Phys. **20**, 367 (1948).

[70] E. E. Salpeter, Phys. Rev. Lett. **28**, 560 (1972).

[71] J. F. Dobson and N. W. Ashcroft, Phys. Rev. B **16**, 5326 (1977).

[72] G. F. Chapline, Phys. Rev. B **6**, 2067 (1972).

[73] A. K. McMahan, Metallic Hydrogen: Recent Theoretical Progress, in *High-Pressure and Low-Temperature Physics*, edited by C. W. Chu and J. A. Woollam (Springer US, Boston, MA, 1978), pp. 21–42.

[74] S. D. Kaim, N. P. Kovalenko, and E. V. Vasiliu, J. Phys. Stud. **1**, 589 (1997).

[75] S. N. Burmistrov and L. B. Dubovskii, Low Temp. Phys. **43**, 1152 (2017).

[76] G. J. Ackland, arXiv:1709.05300.

[77] I. M. Lifshitz and Y. Kagan, Zh. Eksp. Teor. Fiz. **62**, 385 (1972).

[78] M. Eremets, *High Pressure Experimental Methods*, Oxford-Science Publications (Oxford University Press, Oxford, UK, 1996).